AIAA JOURNAL
Vol. 46, No. 9, September 2008

Technical Notes

TECHNICAL NOTES are short manuscripts describing new developments or important results of a preliminary nature. These Notes should not exceed 2500 words (where a figure or table counts as 200 words). Following informal review by the Editors, they may be published within a few months of the date of receipt. Style requirements are the same as for regular contributions (see inside back cover).

Lay-Up Optimization of Composite Stiffened Panels Using Linear Approximations in Lamination Space

J. Enrique Herencia*
University of Bristol,
Bristol, England BS8 1TR, United Kingdom
Raphael T. Haftka†
University of Florida, Gainesville, Florida 32611
and
Paul M. Weaver‡ and Michael I. Friswell§
University of Bristol,
Bristol, England BS8 1TR, United Kingdom

DOI: 10.2514/1.36189

I. Introduction

LAY-UP optimization of composite structures is discrete. The direct application of integer programming (e.g., [1]) or genetic algorithms (GAs) (e.g., [2]) requires large computational resources for demanding structural constraints [e.g., finite element (FE) based], due to the high number of function evaluations involved in the optimization. Alternatively, the use of lamination parameters [3] as design variables enables an efficient continuous optimization (e.g., [4]), although discrete constraints on the laminate stacking sequence cannot be imposed. To overcome this difficulty, a two-step optimization was initially proposed by Yamazaki [5] to maximize the buckling and frequency performance of a composite plate. A gradient-based optimization using lamination parameters as design variables was applied to get near the optimum discrete design. Then, a GA was used to obtain the laminate stacking sequence that most closely matched the lamination parameters from the first step, while satisfying the discrete constraints. Autio [6] followed a similar approach and introduced some lay-up design rules as penalties in the fitness function. An alternative two-step approach was formulated by Todoroki and Haftka [7] to maximize the buckling load of a composite plate. First, continuous optimization of lamination parameters was performed to identify the neighborhood of the optimum discrete design. Next, a response surface approximation was created in that neighborhood and used with a GA to determine the laminate stacking sequence. It was shown that the two-step approach provided good designs with relatively low loss in performance when compared with the global optima.

The authors' previous work [8], based on a two-step approach, was applied successfully to optimize anisotropic composite panels with T-shaped stiffeners. At the first step, continuous optimization of lamination parameters was used to get near the optimum discrete design. The composite stiffened panel was modeled by a single representative skin-stiffener assembly or superstiffener. Figure 1 shows the superstiffener components, geometry, material axis, and positive sign convention for the applied loading. The design variables were the cross-sectional dimensions and lamination parameters of the superstiffener. The design constraints were strength, buckling, and practical design rules. Four stiffener types (a–d), as shown in Fig. 2, were considered in the optimization. At the second step, a GA was used to identify the lay-ups for the superstiffener's laminates, which were the closest in the lamination parameter space to the continuous optima and satisfied the discrete design constraints. However, it was noted that sometimes the optimum discrete designs were not the closest in the lamination parameter space to the continuous optima.

This note seeks to address the problem that the discrete optimum may not be the closest in the lamination parameter space to the continuous optimum. Assuming that the continuous optimum is reasonably close to the discrete optimum, a first-order Taylor series about the continuous optimum is suggested to be sufficient to approximate the design constraints. Thus, a new fitness function based on constraint satisfaction, using the linear approximation of the design constraints, is proposed for the GA to determine the design lay-ups.

II. Optimization Strategy

The optimization strategy shares the first step of gradient-based optimization in the lamination parameter space with [8]. In the second step, however, a GA is used to find the safest design based on a linear approximation of the design constraints, instead of searching for the closest design in the lamination parameter space to the continuous optimum. After the second step, the discrete design is checked using the exact design constraints to verify its feasibility.

A. First Step: Gradient-Based Optimization

As in [8], the first step optimizes a representative element of the stiffened panel or superstiffener using continuous optimization of lamination parameters. Laminates are assumed to be symmetric or midplane symmetric and restricted to 0, 90, 45, and −45 deg ply angles, and thus their properties are characterized by three membrane and three bending lamination parameters. The design constraints are the lamination parameters feasible region, strength, buckling (computed with FE), and practical design rules. Strength constraints are enforced by limiting the superstiffener component strains in x, y, and xy by a strain allowable. Buckling constraints are imposed by not allowing the local and global buckling failures of the superstiffener. Practical design constraints are implemented by limiting the minimum percentages of ply angles in each of the superstiffener component, skin-stiffener Poisson's ratio mismatch, and skin gauge. The objective is to minimize the mass of the superstiffener. The optimum continuous superstiffener's cross-sectional dimensions and

Received 13 December 2007; revision received 28 May 2008; accepted for publication 4 June 2008.

*Marie Curie Research Assistant, Department of Aerospace Engineering, Queen's Building. Student Member AIAA.
†Distinguished Professor, Department of Mechanical and Aerospace Engineering. Fellow AIAA.
‡Reader in Lightweight Structures, Department of Aerospace Engineering, Queen's Building. Member AIAA.
§Sir George White Professor of Aerospace Engineering, Department of Aerospace Engineering, Queen's Building. Member AIAA.

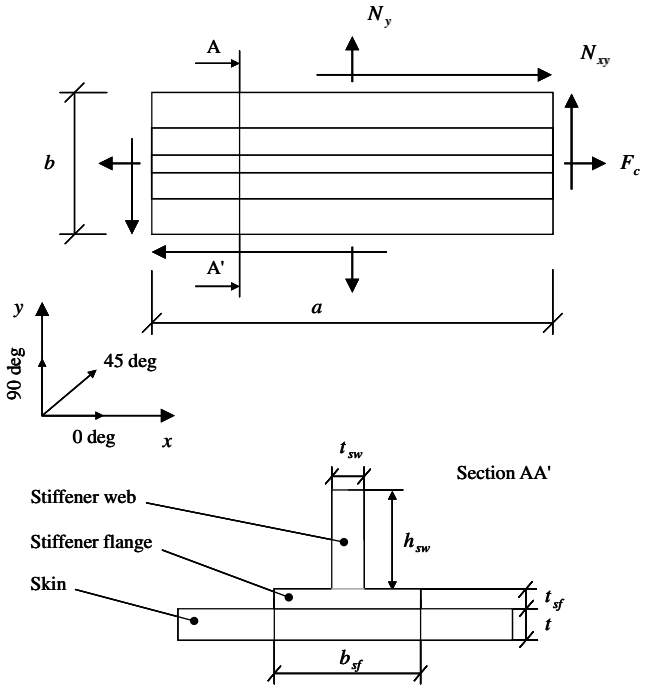

Fig. 1 Superstiffener components, geometry, and loading.

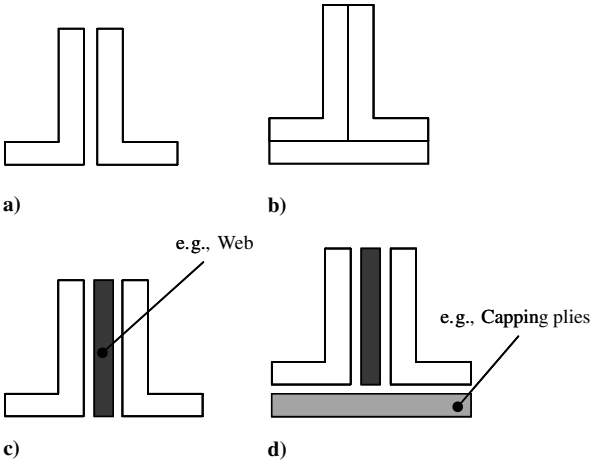

Fig. 2 T-shaped stiffener types manufactured: a) as a back-to-back angle; b) by adding capping plies in the stiffener flange and stiffener web; c) by adding an extra web laminate; d) as a combination of the previous configurations.

lamination parameters are determined. Design constraint sensitivities [9] of the strength, lamination parameters feasible region, and practical design constraints are determined by the forward finite difference approximation with a relative perturbation of 0.0001. Buckling sensitivities are computed in MD NASTRAN [10] via the design sensitivity and optimization solution (SOL 200) [11].

B. Second Step: Genetic-Algorithm-Based Optimization

The second step employs a standard GA similar to that developed in [8] to identify the lay-ups for the superstiffener's laminates. The design constraints are approximated by a first-order Taylor series about the step-1 optimum design. The objective is to find the design with maximum constraint margin. The design variables and encoding scheme for the GA used in this note coincide with those reported in [8]. However, the gene length is longer, as the skin and stiffener lay-ups are determined simultaneously. The fitness function in the GA to be minimized is given by the maximum value obtained from the linear approximation of the design constraints or critical constraint. Thus,

$$G_{\mathrm{cr}}(\boldsymbol{y}) = \max\left\{0, G_j^{\mathrm{opt}} + \sum_{i=1}^{3} \frac{\partial G_j^{(i)}}{\partial \boldsymbol{x}^{(i)}}[\boldsymbol{x}^{(i)} - \boldsymbol{x}^{(i)\mathrm{opt}}]\right\}; \qquad j = 1, \ldots, n_c \tag{1}$$

where $\boldsymbol{y}$ is the gene representing the skin and stiffener lay-ups, G_j^{opt} is the value of the jth constraint for the step-1 optimum design, $G_j^{(i)}$ is the value of the jth constraint for the ith laminate (skin = 1, stiffener flange = 2, and web = 3), $\boldsymbol{x}^{(i)}$ and $\boldsymbol{x}^{(i)\mathrm{opt}}$ are the vectors of design variables for the ith laminate for the discrete and step-1 optimum design, respectively, and n_c is the number of design constraints.

The approximated design constraints are strength, buckling, and practical design rules. Laminate constraints, such as ply contiguity, are applied to each gene by adding extra penalty terms in Eq. (1), as in [8]. Additional laminate constraints, such as locating a set of ± 45 deg plies at the outer surface of the skin and stiffener laminates to improve the laminates' damage tolerance, are also applied following [8].

III. Numerical Examples

An example from [8] is used for direct comparison purposes. Table 1 shows the critical design constraint G_{cr} for the selected example, corresponding to the FE superstiffener designs reported in Table 7 of [8]. Values of $G_{\mathrm{cr}} > 0$ imply constraint violation. Note that the second step of [8] (referred to as old) used a fitness function for the GA based on the squared differences between the lamination parameters for the continuous optimum and discrete design (minimum distance).

The second optimization step described in Sec. II.B (referred to as new) was applied to obtain the lay-ups for the superstiffener's laminates. The thicknesses of the superstiffener's laminates were maintained equal to those in [8] for comparison purposes. The GA used a population of 40, 200 generations, a 0.7 probability of crossover, and a 0.05 probability of mutation. The new optimum superstiffeners obtained from this process are shown in Table 2. Note that M_c and M_d are the masses of the continuous and discrete designs, and λ_b and λ_s are the buckling and strength load factors.

Comparing Table 2 to Table 1, it is seen that the new optimum superstiffener designs improve constraint satisfaction over the closest-lamination-point designs reported in [8], leading to safer constraint margins for three of the four stiffener types. This suggests that the thicknesses of the superstiffener's laminates may be decreased to achieve lighter designs. The new optimum superstiffeners have similar laminates' percentages of ply angles to those reported in [8], but vary their stacking sequences. It is observed that the linear approximation of the design constraints is accurate, except for the design with stiffener type b, where the approximation

Table 1 Critical design constraints for optimum FE superstiffener designs under strength, buckling, practical design, and ply contiguity constraints from [8]

Stiffener type	G_{cr}	Critical design constraint
a	0.008	Skin-stiffener flange Poisson's ratio mismatch
b	0.002	Skin-stiffener flange Poisson's ratio mismatch
c	0.016	Minimum percentage of 90 deg plies in the skin (54.10/36.06/9.84 corresponding to $0/\pm 45/90\%$)
d	−0.013	Strength

Table 2 New optimum superstiffener designs under strength, buckling, practical design, and ply contiguity constraints; linear approximated load factors and critical constraints are shown in parentheses (thicknesses of the superstiffener's laminates as in [8])

Stiffener type	M_c/M_d, kg	λ_b	λ_s	G_{cr}[a]	b_{sf}, mm	h_{sw}, mm	Lay-up	0/ ± 45/90%
a	2.74/2.89	1.027 (1.030)	1.009 (1.017)	−0.004 (−0.001)	60.01	69.95	Skin (59 plies) $[\pm 45/0_2/45/90/\pm 45/0_2/90_2/(\pm 45/0_4)_2/45/0_4/90]_{MS}$ Stiffener (31 plies) $[\pm 45/0/90/0_3/-45/0_4/45/90/0/0]_{MS}$	Skin 54.24/33.90/11.86 Stiffener flange 61.29/25.80/12.90
b	2.74/2.84	1.014 (1.129)	1.013 (1.015)	−0.012 (−0.014)	60.01	69.96	Skin (58 plies) $[\pm 45/(45/0_2)_2/90_2/0_2/(\pm 45)_2/0_2/45/0_2/90/0_4/45/0_2]_S$ Stiffener (47 plies) $[\pm 45/0_4/\pm 45/0_2/-45/0_3/45/0_2/90_2/0_4/90]_{MS}$	Skin 55.17/34.48/10.34 Stiffener 63.83/25.54/10.64
c	2.73/2.89	1.008 (1.062)	1.005 (1.009)	0.008 (0.008)	59.99	69.67	Skin (61 plies) $[\pm 45/45/\pm 45/0_4/90/45/0_4/-45/0/45/90_2/0_4/\pm 45/0_4/90]_{MS}$ Stiffener flange (18 plies) $[\pm 45/-45/45/0_4/90]_S$ Web (32 plies) $[0_4/(90/0_2)_2/0_2/45/0_2/90]_S$	Skin 55.74/32.78/11.48 Stiffener flange 44.44/44.44/11.11 Web 75/6.25/18.75
d	2.73/2.95	1.037 (1.057)	1.021 (1.017)	−0.021 (−0.017)	59.76	69.69	Skin (63 plies) $[\pm 45/90_2/0_2/-45/0_4/\pm 45/0_2/90/0_2/(0_2/45)_2/90/\pm 45/0_2/45/0/0]_{MS}$ Stiffener flange (8 plies) $[\pm 45/90/0]_{MS}$ Web (53 plies) $[0_4/\pm 45/0_4/90/0_2/-45/0_4/90_2/0_4/45/0/0]_{MS}$	Skin 55.56/31.75/12.70 Stiffener flange 25/50/25 Web 73.58/15.10/11.32

[a]Note that for stiffener types a and c, the critical constraint is the skin-stiffener flange Poisson's ratio mismatch, whereas for stiffener types b and d, the critical constraint is strength.

error is about 11% for the buckling load factor. If accuracy becomes an issue, it is possible to update the linear approximation at the step-2 optimum, and conduct one more round of the GA, or to increase the order of the Taylor series. It is noted that the GA produces a vast number of feasible superstiffener designs and that convergence toward the discrete optimum is rapid. Additionally, the new second step usually finds a discrete design that satisfies the step-1 constraints in one run of the GA. In contrast, the old step needed to run the GA a few times to obtain a feasible design.

The design space is 14-dimensional for stiffener types a–b and 21-dimensional for stiffener types c–d. To visualize the difference between the old and new superstiffener designs in this high-dimensional space, the technique of Knill et al. [12] was employed, and a plane defined by the step-1 optimum and the old and new step-2 optima was generated. Figure 3 provides a graphical representation of the distances (scaled) between optima and shows examples of contour maps of the critical constraint in that plane for stiffener type a. Note that some of the design points in the plane may not actually correspond to possible laminates, as they may not have an integer number of plies. Laminates with an integer number of plies may lie above or below the plane. From this figure, it is clearly seen that the new discrete optima are further away and in a substantially different direction from the step-1 designs but have lower constraint violation. For example, for the skin laminate, the minimum-distance approach finds a design at a distance of 0.0485 in the lamination parameter space, whereas the new distance is 0.2695. The angle

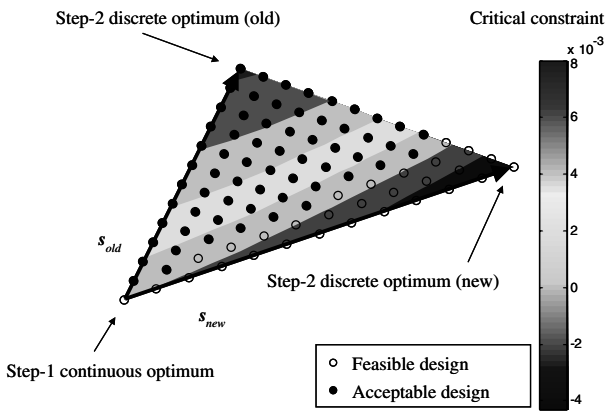

Fig. 3 Critical constraint contour plot for stiffener type a. Feasible design points are represented by open circles, whereas those slightly (under 0.02), violating some constraints but still acceptable, are shown by full circles. The old and new search directions are S_{old} and S_{new}.

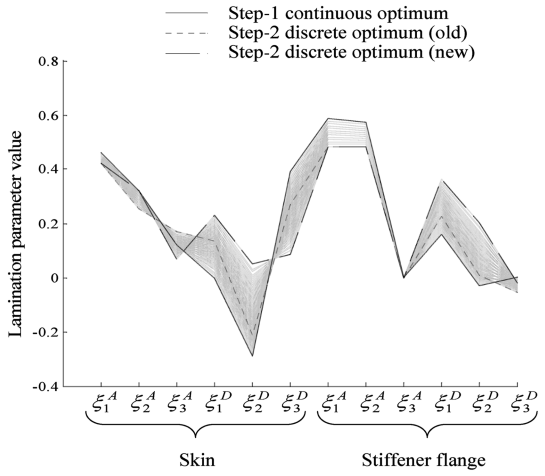

Fig. 4 Lamination parameters for stiffener type a: ξ_i^A and ξ_i^D are the ith membrane and bending lamination parameters, respectively ($i = 1, 2, 3$) (e.g., [3]). The lamination parameters corresponding to each of the designs contained within the plane of Fig. 3 are shown in gray shading.

Table 3 New optimum superstiffener designs under strength, buckling, practical design, and ply contiguity constraints; linear approximated load factors and critical constraints are shown in parentheses

Stiffener type	M_c/M_d, kg	λ_b	λ_s	G_{cr}[a]	b_{sf}, mm	h_{sw}, mm	Lay-up	0/ ± 45/90%
a	2.74/2.79	0.991 (0.996)	0.989 (0.991)	0.011 (0.009)	60.01	69.95	Skin (58 plies) $[(\pm45)_3/90_2/0_2/45/0_4/\pm45/0_4/45/0_4/90/0_2]_S$ Stiffener (29 plies) $[\pm45/45/0_4/-45/0_4/90/0/90]_{MS}$	Skin 55.17/34.48/10.34 Stiffener flange 62.07/27.58/10.34
c	2.73/2.82	0.982 (1.000)	0.989 (0.992)	0.018 (0.000)	59.99	69.67	Skin (63 plies) $[\pm45/90_2/0/45/90/0_2/45/\pm45/0_4/45/0_4/(-45/0_2)_2/90/\pm45/0/0]_{MS}$ Stiffener flange (14 plies) $[\pm45/0_4/90]_S$ Web (31 plies) $[0_4/-45/0_4/45/0_4/90/0]_{MS}$	Skin 52.38/34.92/12.70 Stiffener flange 57.14/28.58/14.29 Web 80.65/12.90/6.45
d	2.73/2.91	1.028 (1.040)	1.001 (1.004)	−0.001 (−0.004)	59.76	69.69	Skin (63 plies) $[\pm45/90/-45/0_4/45_2/90_2/0_2/-45/0_2/(\pm45/0_4)_2/90/0/0]_{MS}$ Stiffener flange (7 plies) $[\pm45/90/0]_{MS}$ Web (53 plies) $[0_2/45/(0_4/90)_2/90/0_4/\pm45/0_4/-45/0/0]_{MS}$	Skin 55.56/31.74/12.70 Stiffener flange 14.29/57.14/28.57 Web 73.58/15.10/11.32

[a]Note that the critical constraint for stiffener types a and d is strength, whereas for stiffener type c, the critical constraint is buckling.

between the minimum distance and new design directions is 53.21 deg. For the stiffener laminate, the trend is similar and the minimum-distance approach finds a design at a distance of 0.0271 in the lamination parameter space; in contrast, the new distance is 0.1135 and the angle between the minimum distance and new design directions is 68.16 deg. Further details and examples can be found in [13].

Figure 4 shows in parallel coordinates the lamination parameters of the superstiffener designs for stiffener type a within the plane represented in Fig. 3. Although there seem to be similarities in the values of the membrane lamination parameters, it is clearly seen that the step-2 optima do not match the lamination parameters of the step-1 optima, and thus are not close to step-1 optima in the lamination parameter space. Additional examples can be found in [13].

Finally, and as a consequence of lower critical constraint violation of the designs presented in Table 2, it was possible to reduce the thicknesses of the superstiffener's laminates. The new second optimization step was applied as before to obtain the lay-ups for the skin and stiffener but allowing the thicknesses of the superstiffener's laminates to vary from those in [8]. The new optimum superstiffeners obtained are shown in Table 3.

The laminates of the new optimum superstiffeners listed in Table 3 differ slightly in percentages of ply angles and possess a different stacking sequence from those in Table 2 and from those reported in [8]. Note that stiffener type b design is not shown, as no feasible design was found by decreasing the thicknesses of the superstiffener's laminates. The new optimum superstiffener designs offer a potential mass saving of approximately 3.5, 2.4, and 1.4% for stiffener types a, c, and d, respectively, when compared with those in Table 2 and those reported in [8]. As in the preceding example, the GA generates a large number of feasible superstiffener designs with very rapid convergence toward the discrete optimum, and a design that satisfies the step-1 constraints was usually found after running the GA only once.

Details of the thicknesses and lamination parameters for the step-1 optimum and the old and new step-2 optima for the examples presented in this note, as well as the lamination distances and angle between search directions, can be found in [13].

IV. Conclusions

Finding a nearby design with continuous optimization as a first step is a standard approach for reducing the cost of discrete optimization. The authors' previous work on the design of composite stiffened panels used lamination parameters for this first step, and then sought the discrete design that was the closest in lamination parameter space to the continuous design (minimum-distance approach). In this note, a new second-step optimization that used a GA to find the safest design based on a first-order Taylor series about the continuous optimum was developed.

For the same thicknesses of the laminates, the new second step generated designs with lower critical constraint violation than those found using the minimum-distance approach. This was used to further reduce the thicknesses of the laminates. It was found that the new second step produced optimum discrete designs with a potential mass saving of 3.5% corresponding to stiffener type a. Furthermore, it was observed that the new optimum discrete designs were further away and in a substantially different direction, and thus were not close in the lamination parameter space to the continuous optima.

The first-order Taylor series approximated the design constraints well, showing a maximum deviation of approximately 11% for the buckling load factor. However, accuracy can be improved by updating the linear approximation at the second-step optimum and conducting one more round of the GA or by increasing the order in the Taylor series. The use of a fitness function based on a linear approximation in the second step is particularly useful when expensive design constraints (e.g., FE based) are employed. Less expensive constraints (e.g., closed-form solutions) may be used directly to form the fitness function.

Acknowledgments

The authors thank the European Commission for the Marie Curie Excellence Grant MEXT-CT-2003-002690. The first author would like to thank Mark Bloomfield for his general comments.

References

[1] Haftka, R. T., and Walsh, J. L., "Stacking Sequence Optimization for Buckling of Laminated Plates by Integer Programming," *AIAA Journal*, Vol. 30, No. 3, 1992, pp. 814–819. doi:10.2514/3.10989

[2] Nagendra, S., Haftka, R. T., and Gürdal, Z., "Design of a Blade Stiffened Composite Panel by a Genetic Algorithm," AIAA Paper 93-1584-CP, 1993.

[3] Tsai, S. W., and Hahn, H. T., *Introduction to Composite Materials*, Technomic, Lancaster, PA, 1980.
[4] Miki, M., and Sugiyama, Y., "Optimum Design of Laminated Composite Plates Using Lamination Parameters,". AIAA Paper 91-0971-CP, 1991.
[5] Yamazaki, K., "Two-Level Optimization Technique of Composite Laminate Panels by Genetic Algorithms," AIAA Paper 96-1539-CP, 1996.
[6] Autio, M., "Determining the Real Lay-Up of a Laminate Corresponding to Optimal Lamination Parameters by Genetic Search," *Structural and Multidisciplinary Optimization*, Vol. 20, No. 4, 2000, pp. 301–310. doi:10.1007/s001580050160
[7] Todoroki, A., and Haftka, R. T., "Lamination Parameters for Efficient Genetic Optimization of the Stacking Sequences of Composite Panels," AIAA Paper 98-4816, 1998.
[8] Herencia, J. E., Weaver, P. M., and Friswell, M. I., "Optimization of Long Anisotropic Laminated Fibre Composite Panels with T-Shaped Stiffeners," *AIAA Journal*, Vol. 45, No. 10, 2007, pp. 2497–2509. doi:10.2514/1.26321
[9] Vanderplaats, G. N., *Numerical Optimization Techniques for Engineering Design*, 3rd ed., Vanderplaats Research & Development, Colorado Springs, CO, 2001.
[10] MD NASTRAN Software Package, Ver. 2006r1, MSC Software, Santa Ana, CA, 2006.
[11] Johnson, E. H., MSC/NASTRAN Design Sensitivity and Optimization, User's Guide, MSC Software, Santa Ana, CA, 2005.
[12] Knill, D. L., Giunta, A. A., Baker, C. A., Grossman, B., Mason, W. H., Haftka, R. T., and Watson, L. T., "Response Surface Models Combining Linear and Euler Aerodynamics for Supersonic Transport Design," *Journal of Aircraft*, Vol. 36, No. 1, 1999, pp. 75–86.
[13] Herencia, J. E., Haftka, R. T., Weaver, P. M., and Friswell, M. I., "Optimization of Anisotropic Composite Panels with T-Shaped Stiffeners Using Linear Approximations of the Design Constraints to Identify Their Stacking Sequences," *7th ASMO-UK Conference* [CD-ROM], 2008.

R. Kapania
Associate Editor